Supplement of

Aerodynamic gradient flux measurements of ammonia in intensively grazed grassland: temporal variations, environmental drivers, methodological challenges and uncertainties

Mubaraq Olarewaju Abdulwahab[1], Christophe Flechard[1], Yannick Fauvel[1], Christoph Häni[2], Adrien Jacotot[1,a], Anne-Isabelle Graux[3] , Nadège Edouard[3] , Pauline Buysse[1], Valérie Viaud[1] , Albrecht Neftel[4]

[1] UMR 1069 SAS, INRAE, Institut Agro, Rennes, 35042, France
[2]School of Agricultural, Forest and Food Sciences HAFL, Bern University of Applied Sciences, Zollikofen, 3052, Switzerland
[3]UMR PEGASE, INRAE, Institut Agro, Saint-Gilles, 35590, France
[4]Neftel Research Expertise, Wohlen b. Bern, 3033, Switzerland
[a]now at: CarboFlux, France

Correspondence to: Mubaraq Olarewaju Abdulwahab (mubaraq-olarewaju.abdulwahab@inrae.fr)

Contents

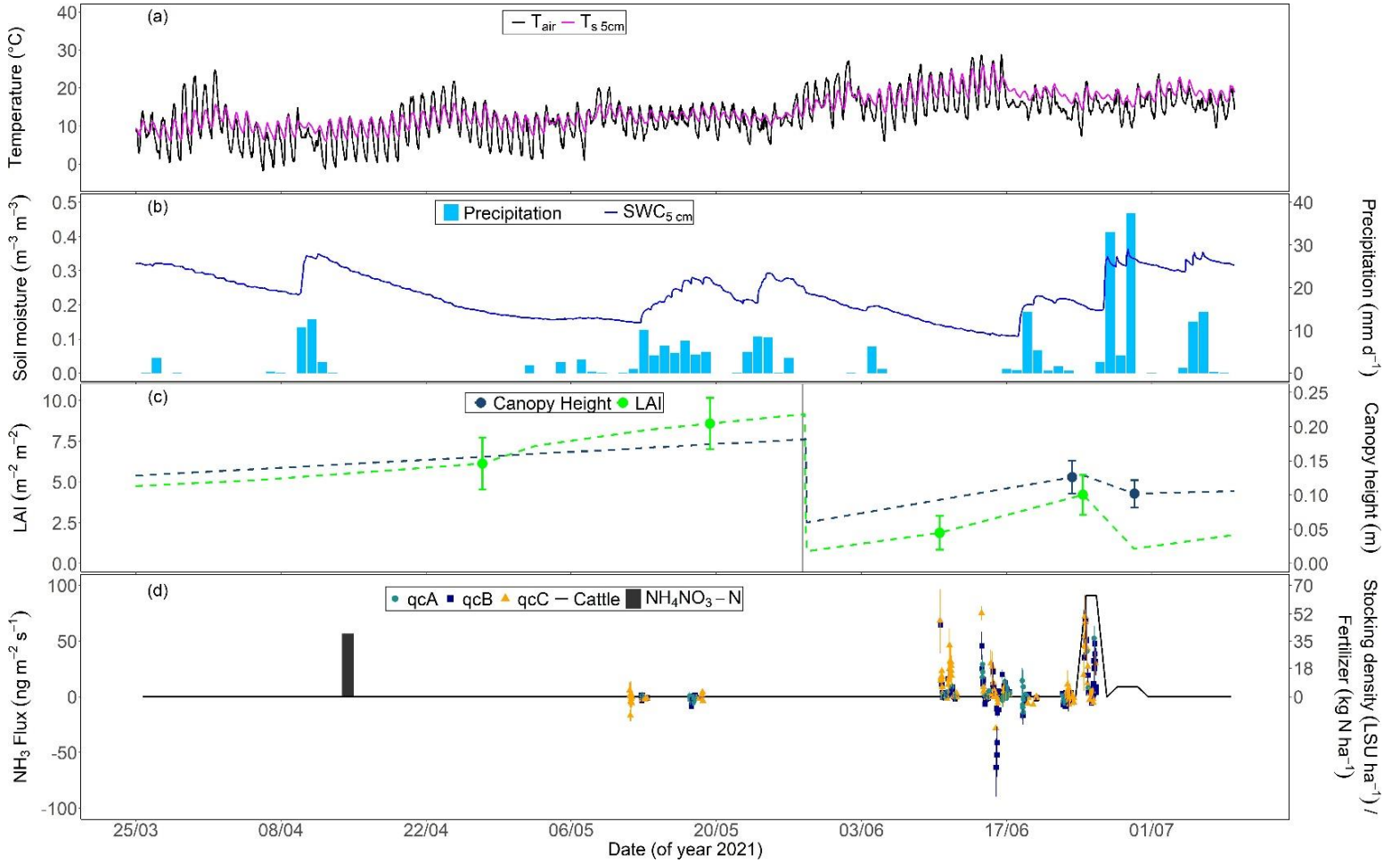

Figure S1: Time series of measured NH_3 fluxes, environmental conditions, and management events during spring 2021 for plot A. (a) Air temperature and soil temperature at 5 cm depth. (b) Precipitation and soil moisture at 5 cm depth. (c) Leaf area index (LAI) and canopy height. (d) NH_3 fluxes are categorized by quality classes (qcA, qcB and qcC, as defined in the main text), alongside stocking density (black line) and fertilizer application (black bars). Grass cuts are shown only for 2021, as no cutting occurred in subsequent years.

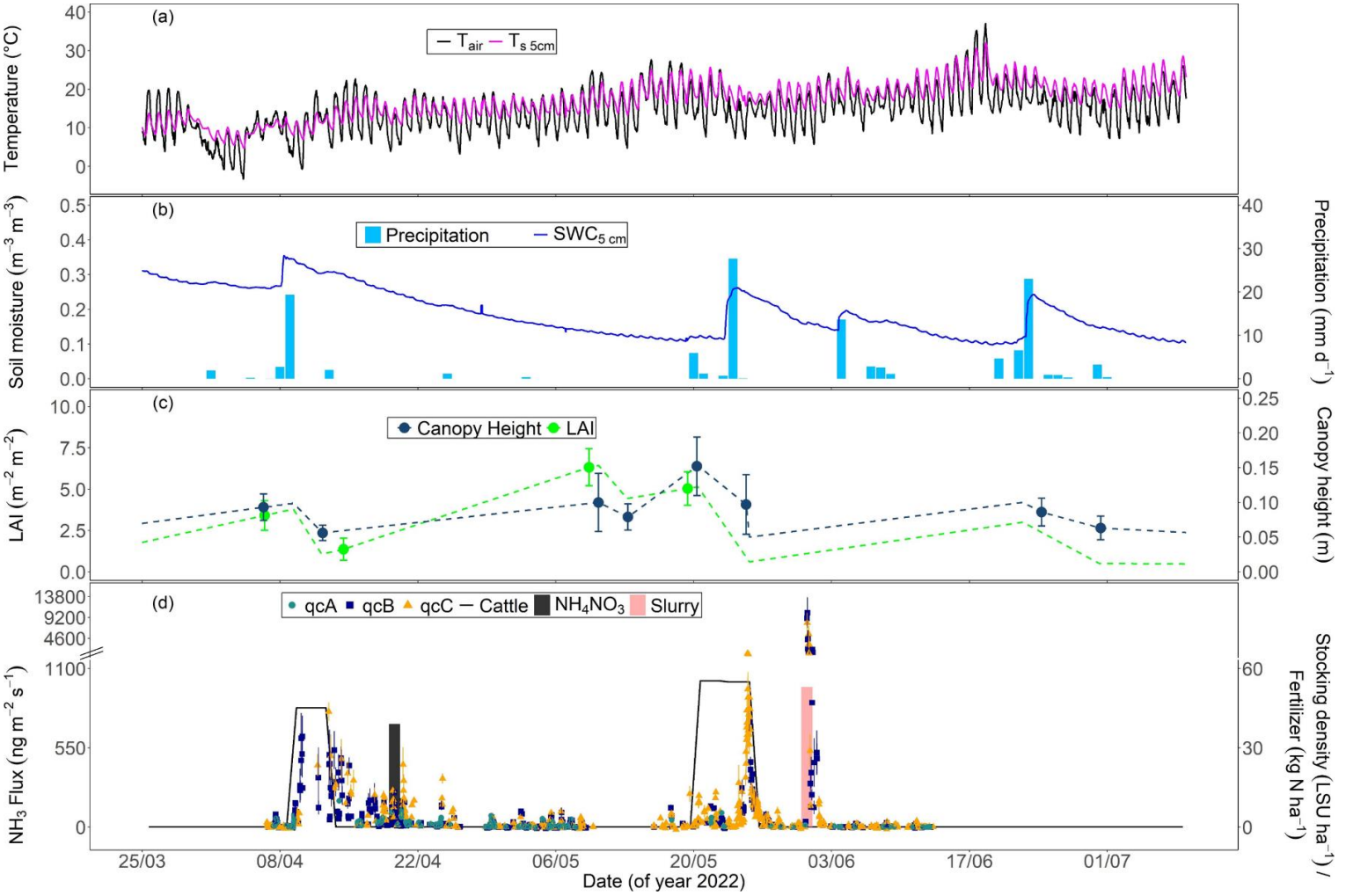

Figure S2: Time series of measured NH_3 fluxes, environmental conditions, and management events during spring 2022 for plot A. (a) Air temperature and soil temperature at 5 cm depth. (b) Precipitation and soil moisture at 5 cm depth. (c) Leaf area index (LAI) and canopy height. (d) NH_3 fluxes are categorized by quality classes (qcA, qcB and qcC, as defined in the main text), alongside stocking density (black line) and fertilizer application (black and pink bars).

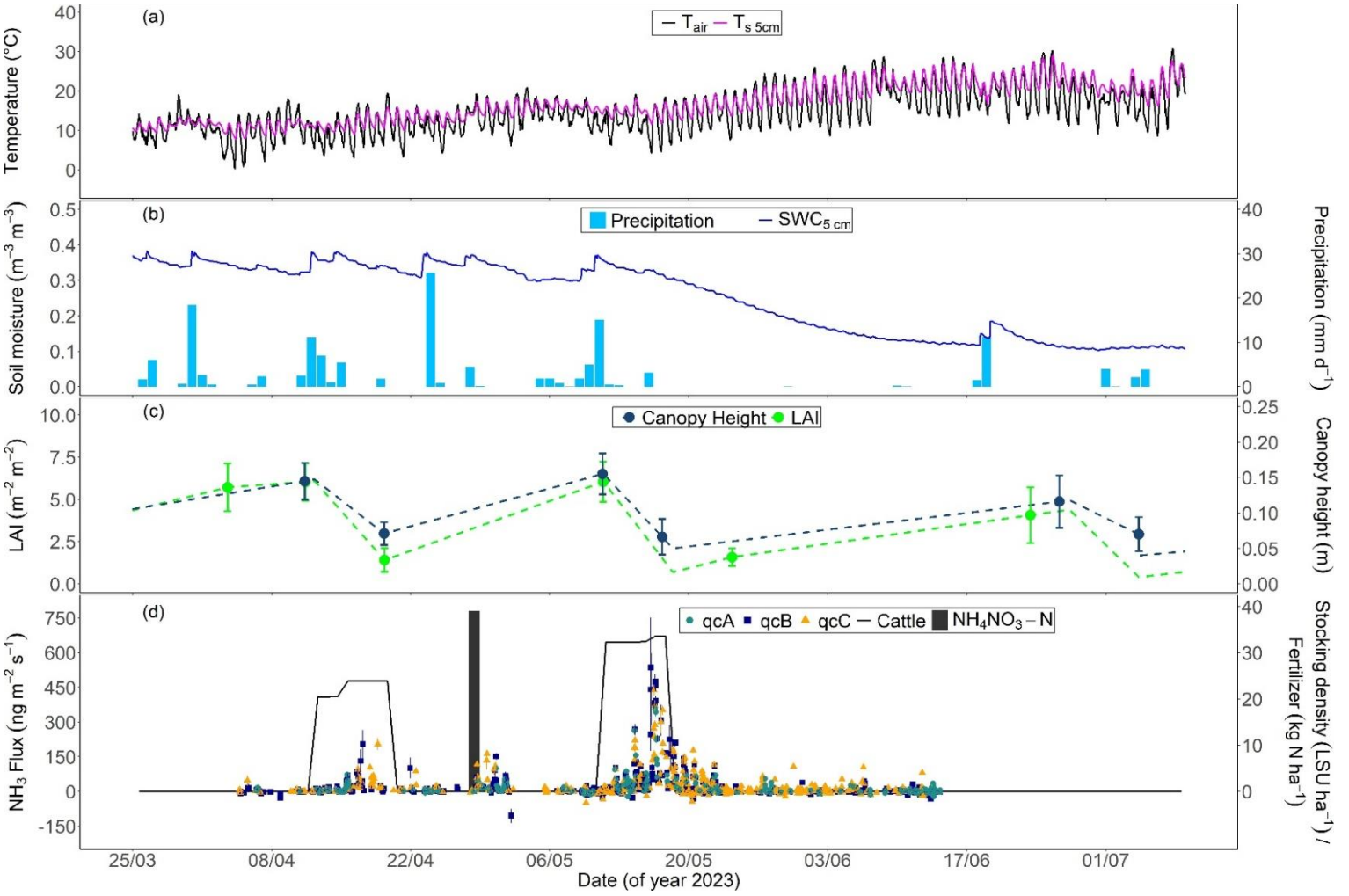

Figure S3: Time series of measured NH_3 fluxes, environmental conditions, and management events during spring 2023 for plot A. (a) Air temperature and soil temperature at 5 cm depth. (b) Precipitation and soil moisture at 5 cm depth. (c) Leaf area index (LAI) and canopy height. (d) NH_3 fluxes are categorized by quality classes (qcA, qcB and qcC, as defined in the main text), alongside stocking density (black line) and fertilizer application (black and pink bars).

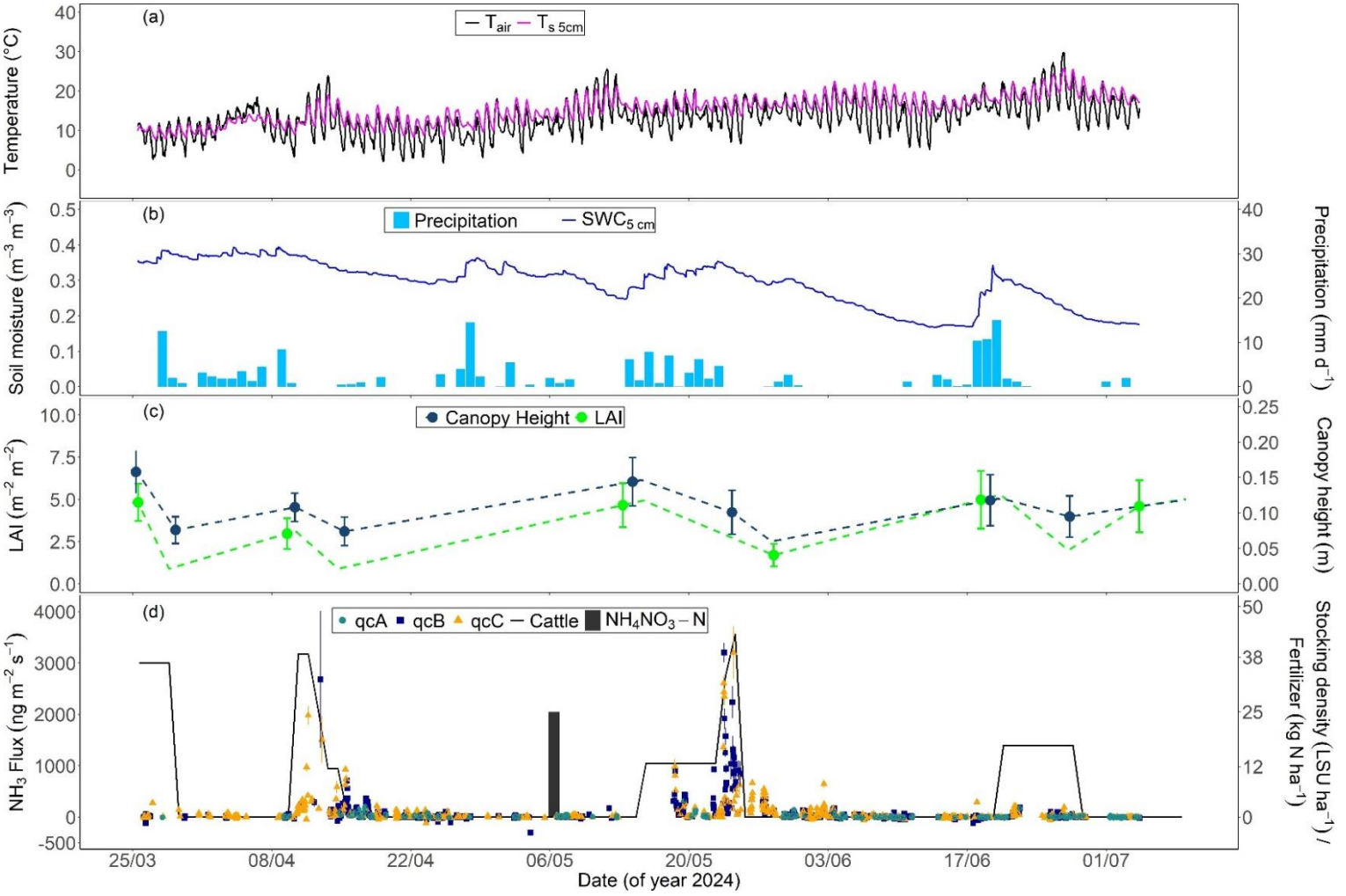

Figure S4: Time series of measured NH_3 fluxes, environmental conditions, and management events during spring 2024 for plot A. (a) Air temperature and soil temperature at 5 cm depth. (b) Precipitation and soil moisture at 5 cm depth. (c) Leaf area index (LAI) and canopy height. (d) NH_3 fluxes are categorized by quality classes (qcA, qcB and qcC, as defined in the main text), alongside stocking density (black line) and fertilizer application (black bars).

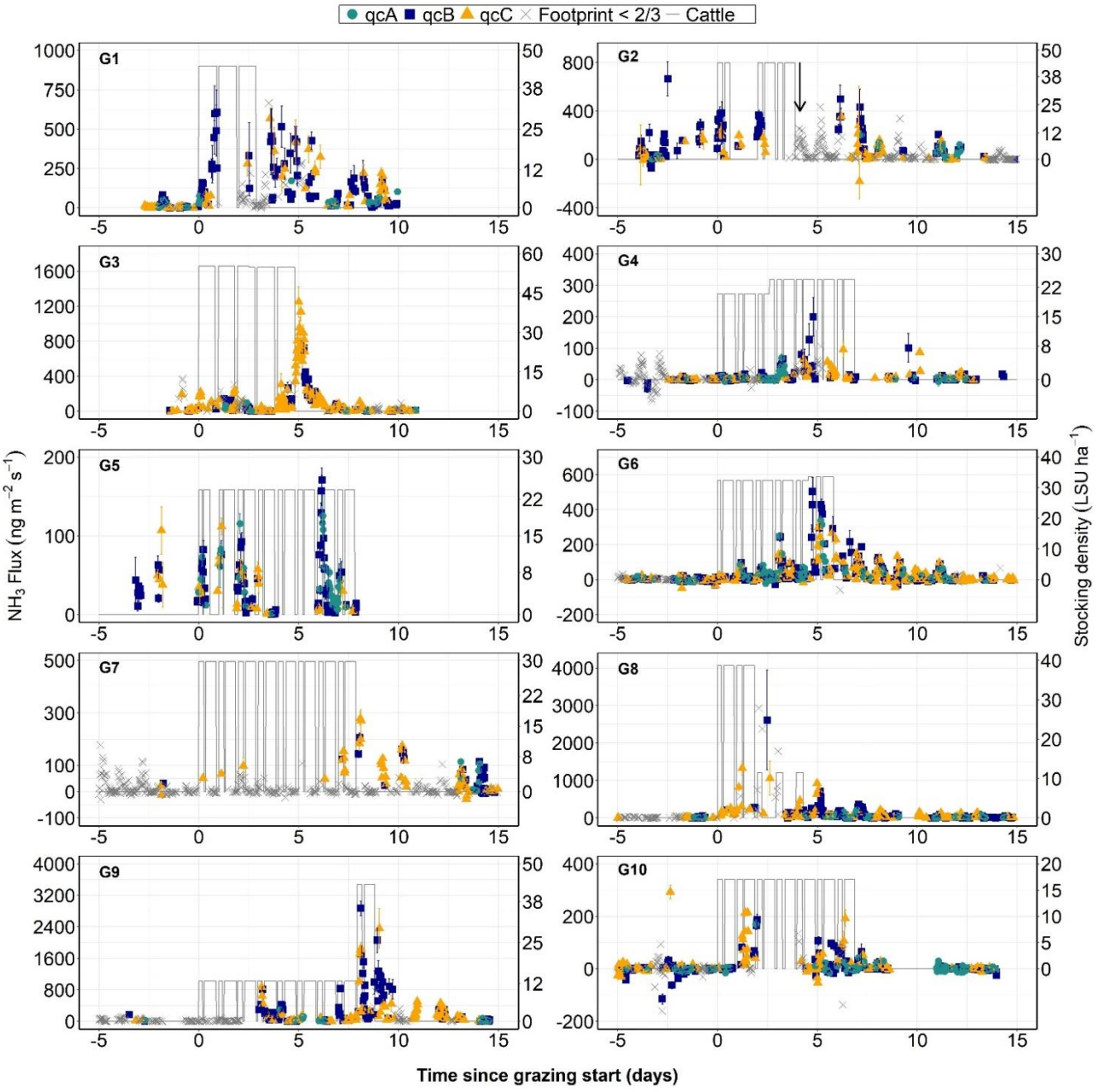

Figure S5: Temporal patterns of grazing-induced NH_3 fluxes (symbols) and stocking density (grey lines), measured up to 15 days after the onset of grazing for the 10 events summarized in Table 2 in the main article. Coloured symbols (green circles, blue squares, orange triangles) show NH_3 fluxes not corrected for footprint for the plot of interest in three quality classes (qcA, qcB and qcC), respectively, as defined in the main text, with error bars showing random errors calculated from Eq. 10 in the main text. Grey crosses indicate fluxes that were micrometeorologically valid but for which the required footprint criteria (> 2/3) were not satisfied. The arrow in G2 indicates a fertilization application of 39 kg NH_4NO_3-N ha^{-1} that occurred just after grazing ended. Note that different y-axis scales are used due to variations in flux magnitude between grazing events.

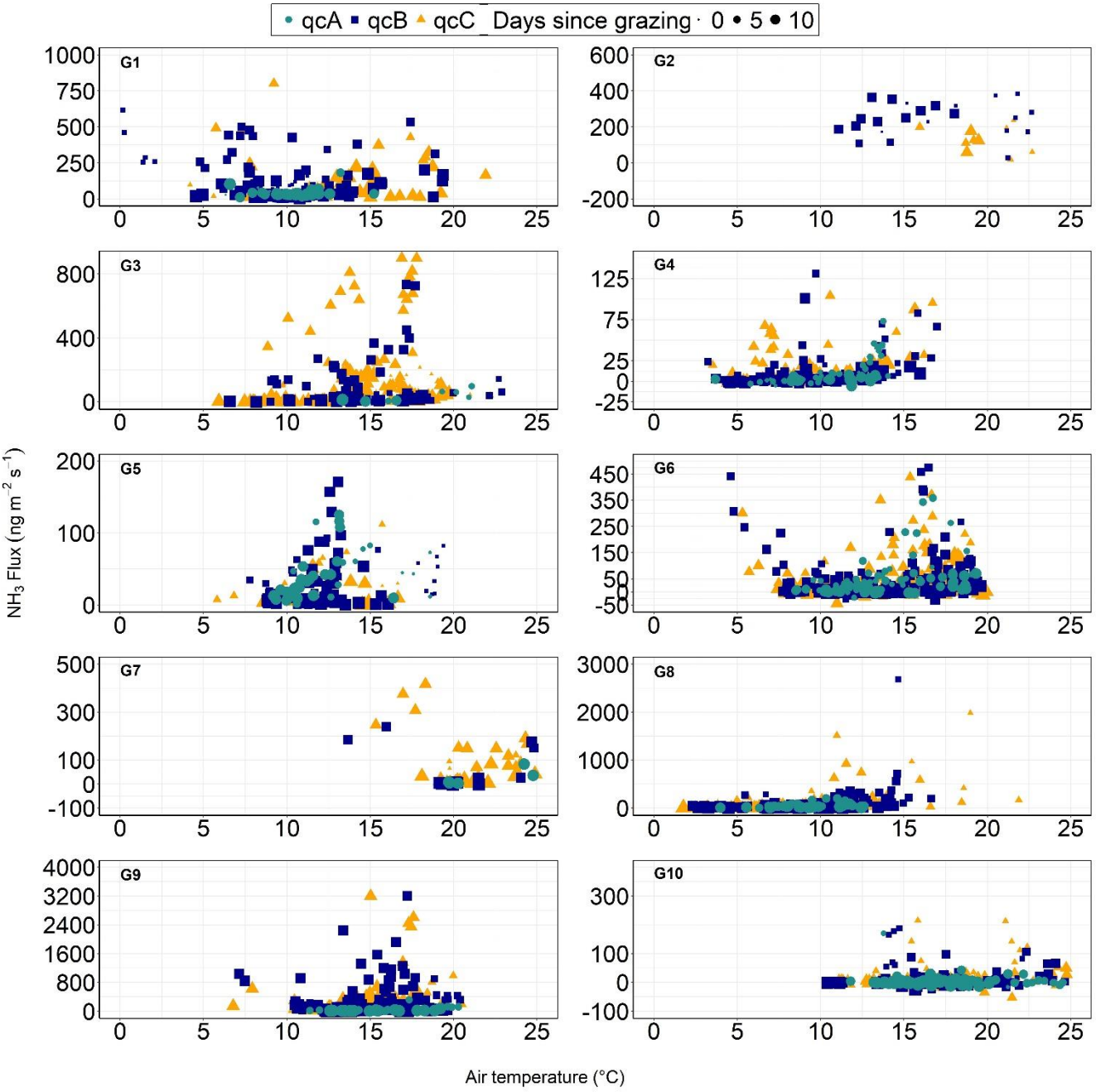

Figure S6: Relationship between NH_3 fluxes and air temperature for grazing events G1-G10. Half-hourly fluxes are shown. Symbol sizes correspond to the time elapsed since the grazing event started.

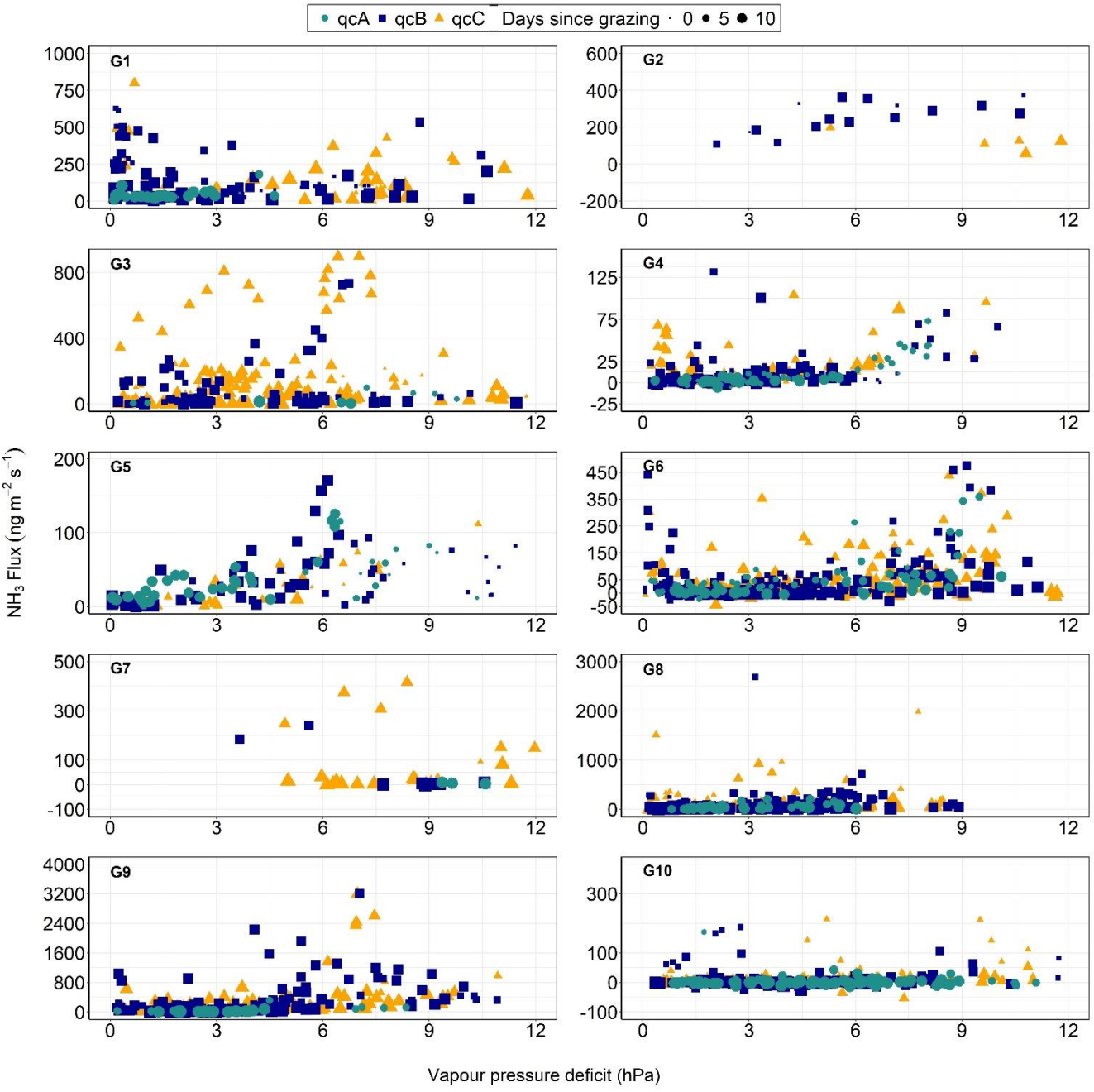

Figure S7: Relationship between NH_3 fluxes and VPD for grazing events G1-G10. Half-hourly fluxes are shown. Symbol sizes correspond to the time elapsed since the grazing event started.

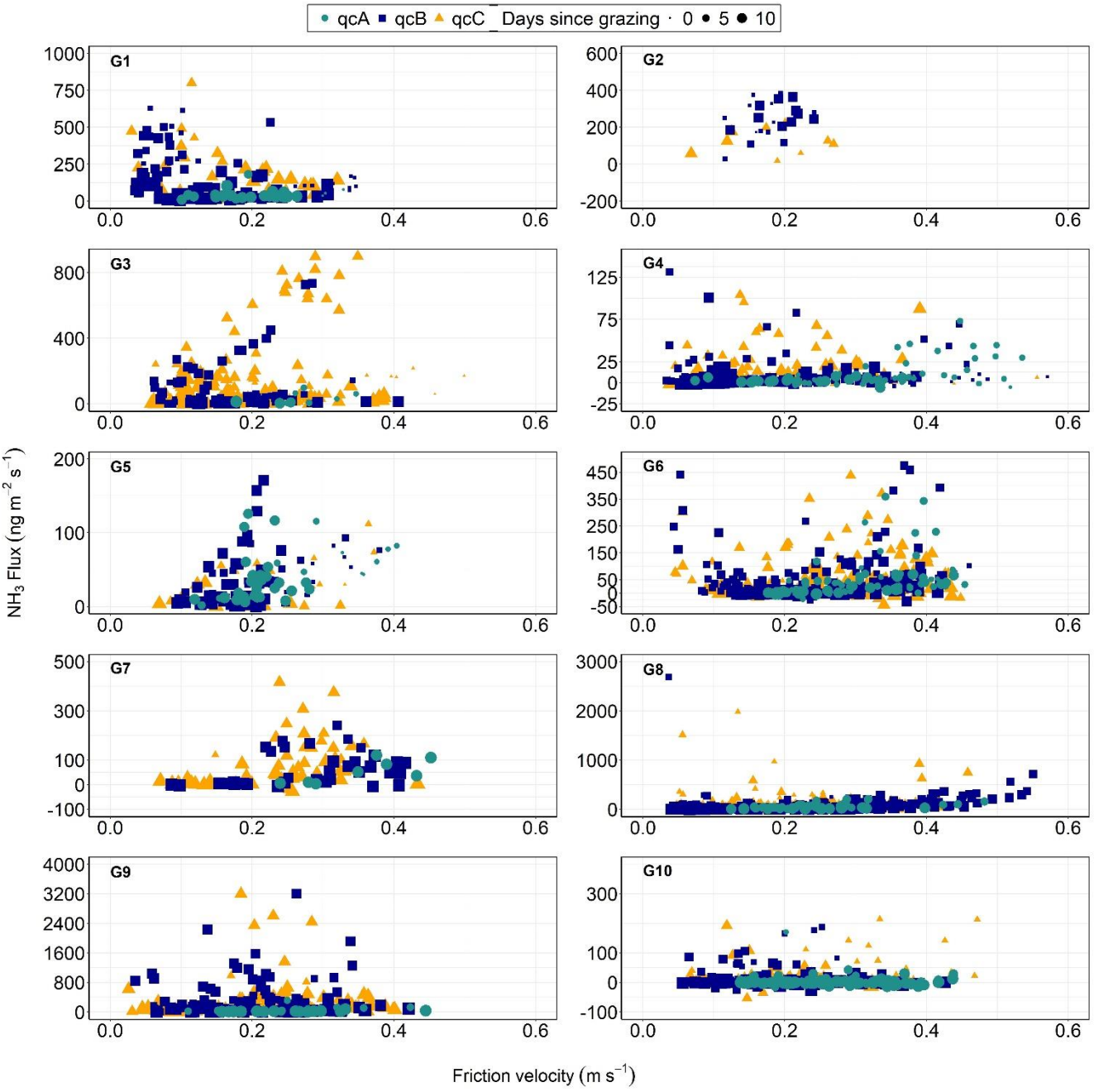

45

Figure S8: Relationship between NH_3 fluxes and friction velocity(u*) for grazing events G1-G10. Half-hourly fluxes are shown. Symbol sizes correspond to the time elapsed since the grazing event started.

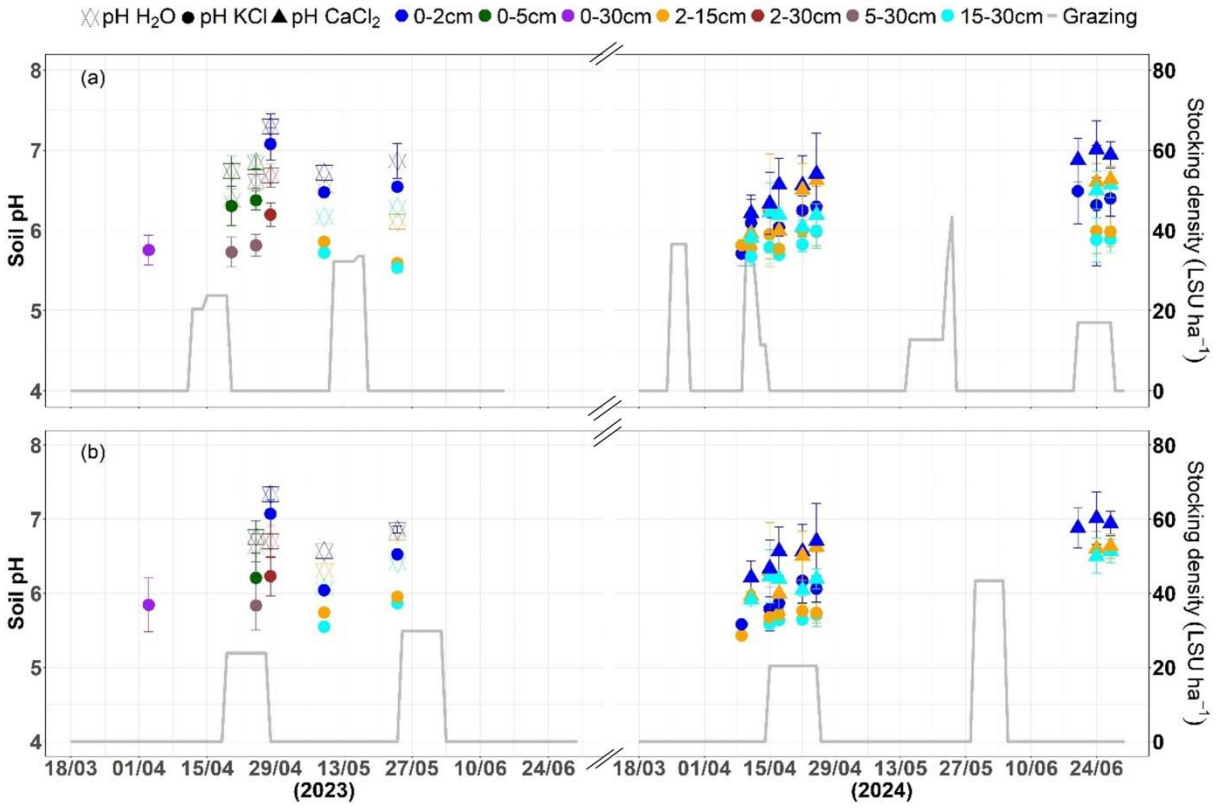

Figure S9: Soil pH variation across different soil depths (0–30 cm) in relation to grazing activity in 2023 and 2024 for (a) Plot A and (b) Plot B. Error bars denote standard deviations across replicates.

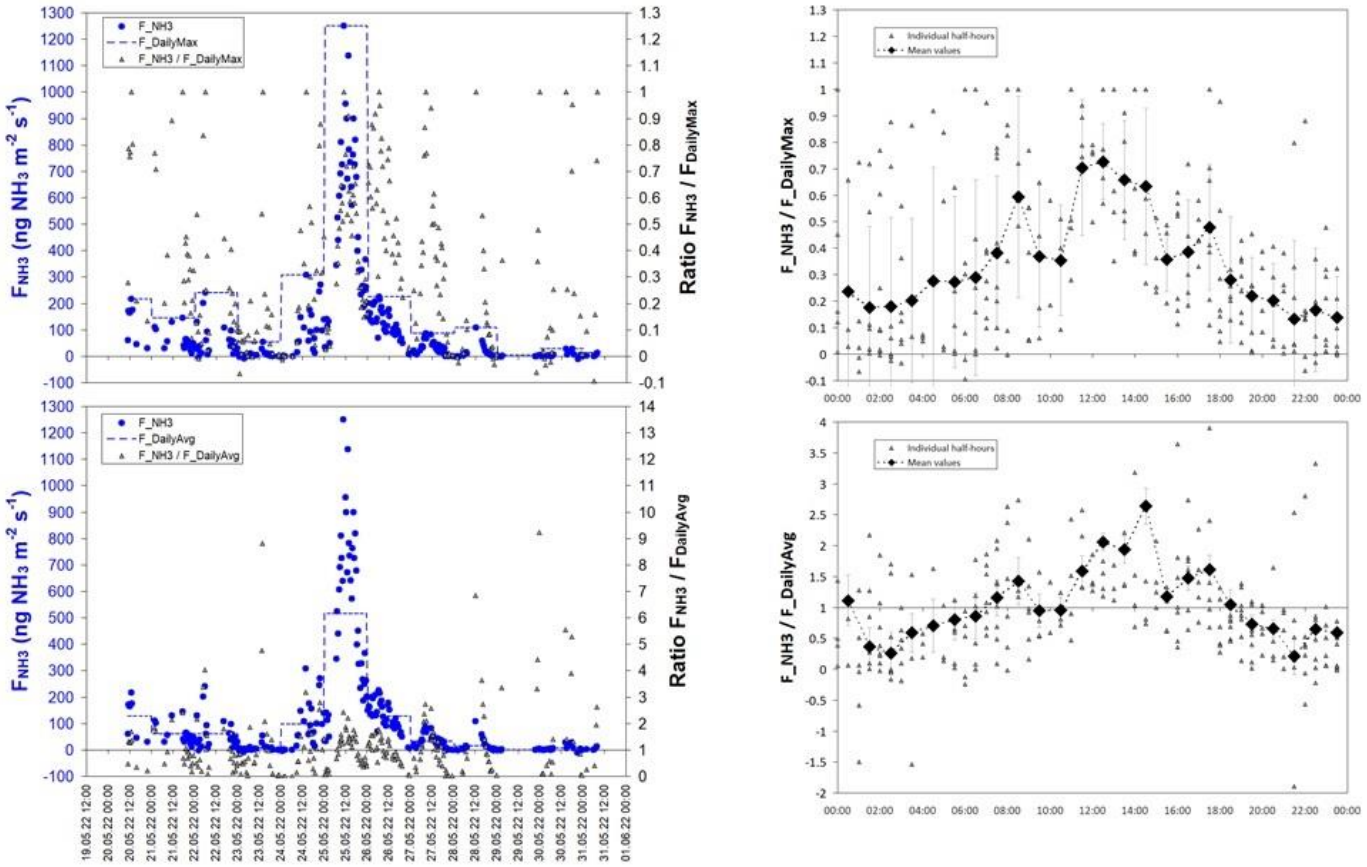

Figure S10: Example calculations for grazing period G3 of the mean diurnal flux patterns, with top: DVmax and bottom: DVavg (see equations 12 in the main article).

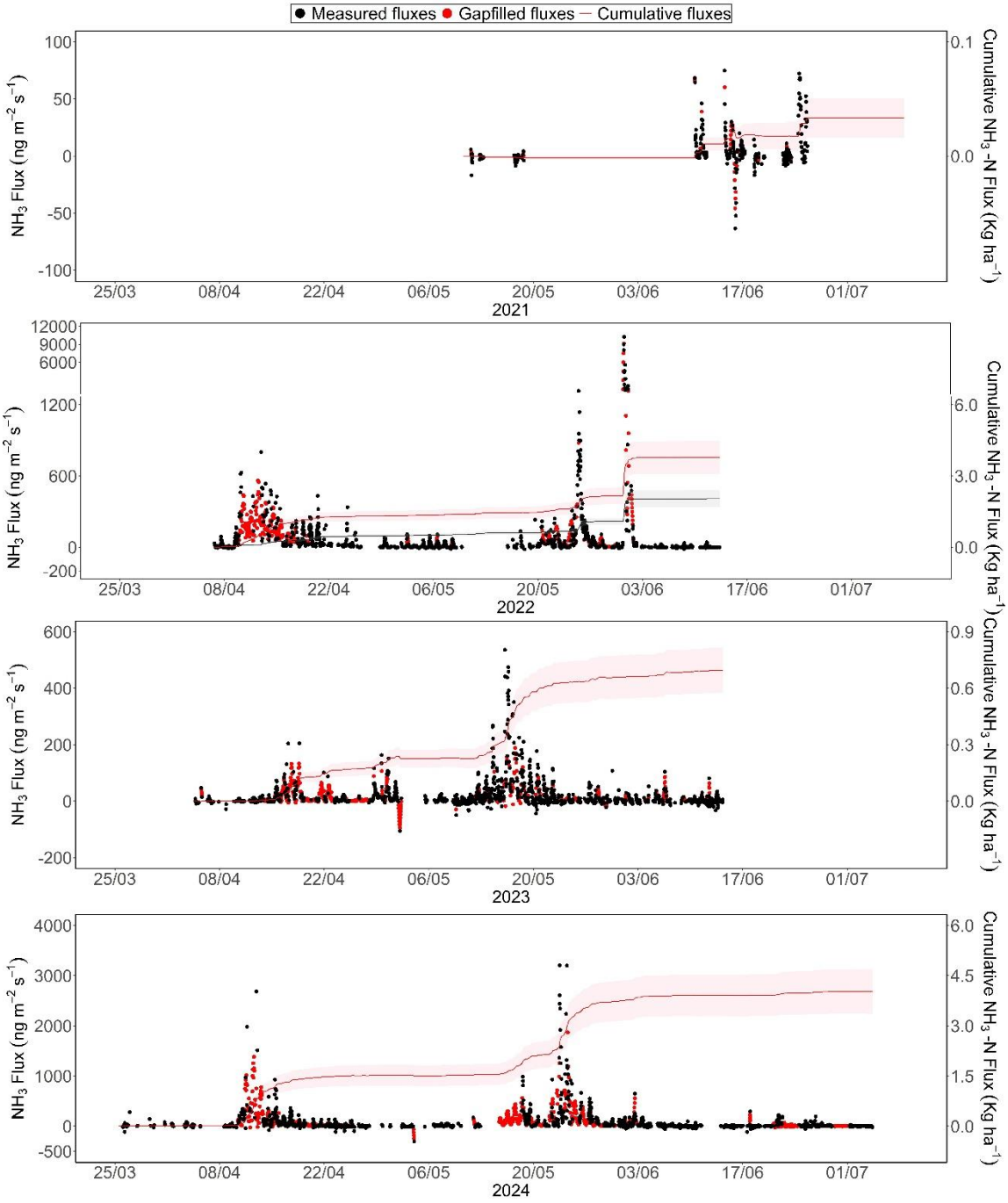

Figure S11: Measured (black) and gap-filled (red) NH_3 fluxes and cumulative emissions for 2021–2024 in Plot A. Gap-filling was performed using linear interpolation outside grazing periods and the DVmax method during grazing (see section 2.6 in the main text). The red lines indicate cumulative emissions over the season. Red-shaded areas indicate uncertainty in cumulative NH_3 flux estimates.

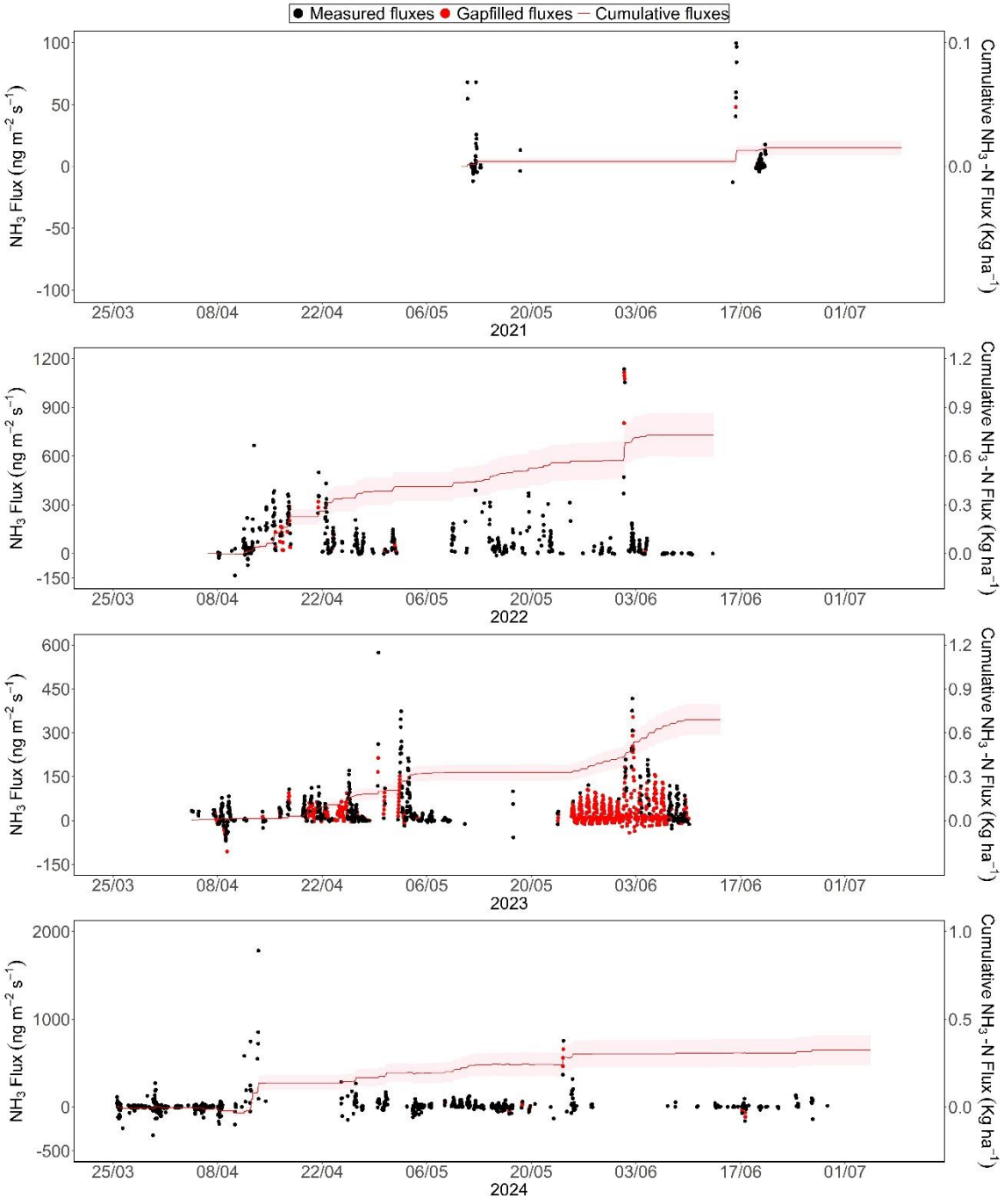

Figure S12: Measured (black) and gap-filled (red) NH_3 fluxes and cumulative emissions for 2021–2024 in Plot B. Gap-filling was performed using linear interpolation outside grazing periods and the DVmax method during grazing (see section 2.6 in the main text). The red lines indicate cumulative emissions over the season. Red-shaded areas indicate uncertainty in cumulative NH_3 flux estimates.

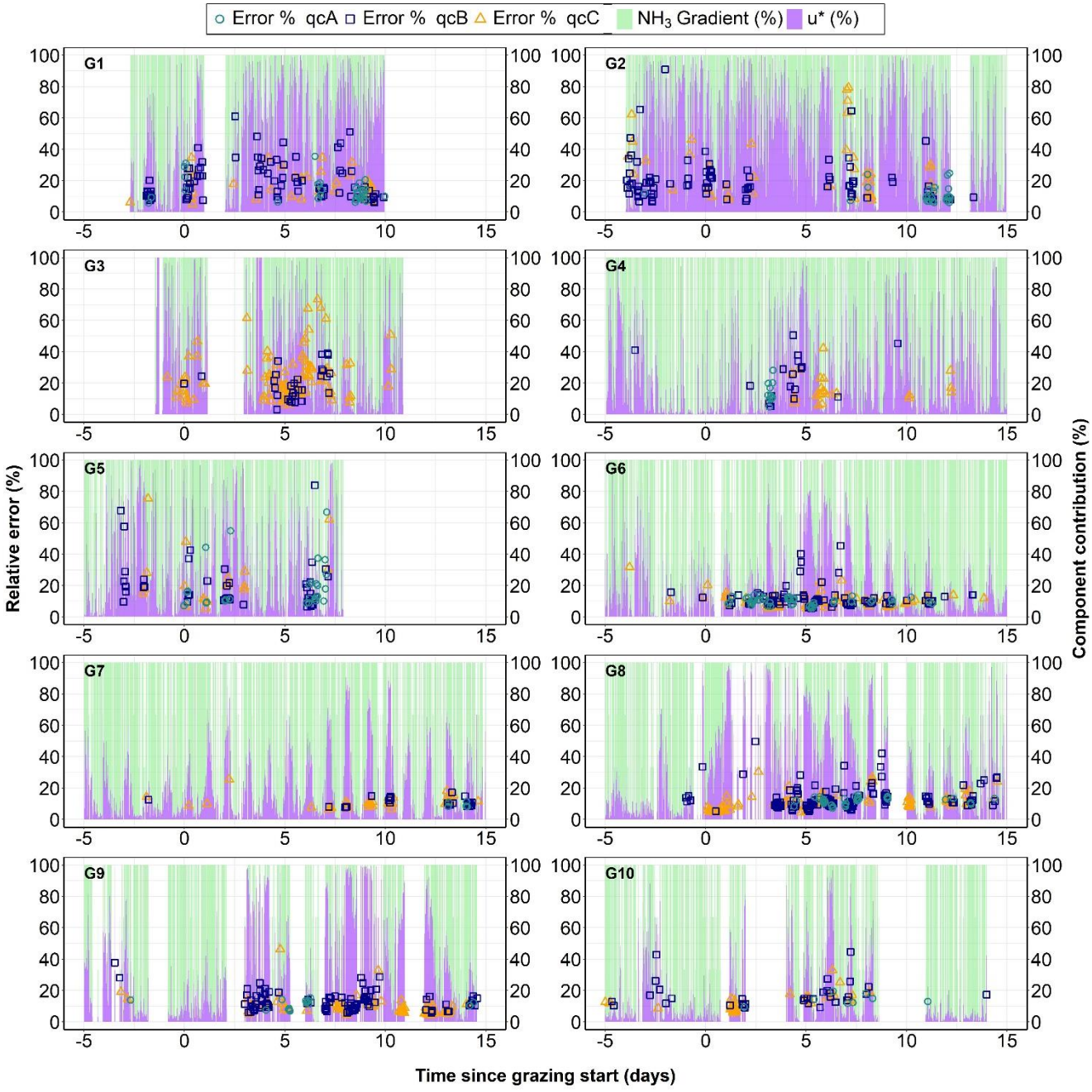

Figure S13: Relative random errors (%) in NH_3 flux measurements across grazing events G1–G10. Coloured markers represent flux quality classes: qcA (circles), qcB (squares), and qcC (triangles). The background shaded areas indicate the contributions of NH_3 concentration gradients (green) and friction velocity u* (purple) to overall flux uncertainty.

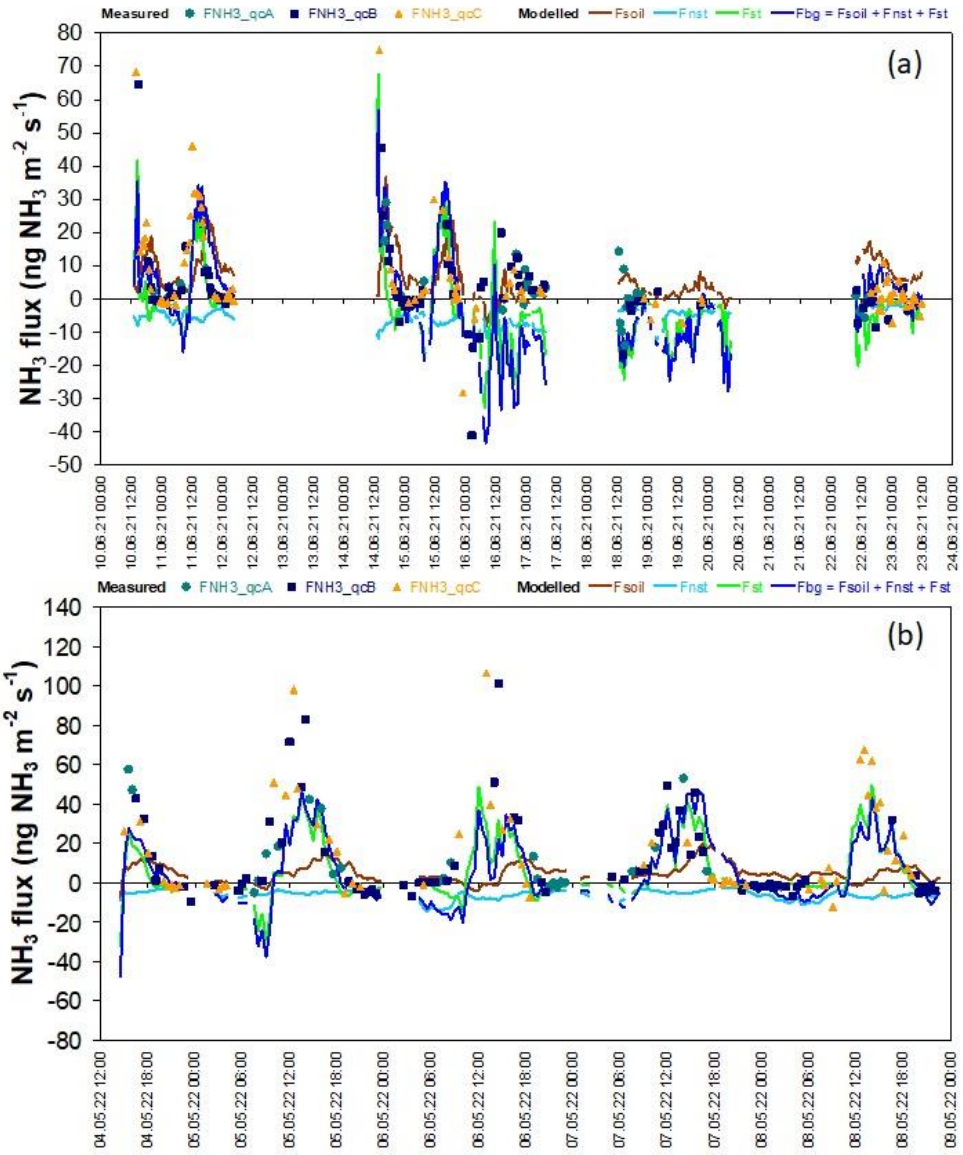

Figure S14: Example bi-directional NH_3 flux data measured in background conditions (well outside of grazing or fertilization periods) in springs 2021 (a) and 2022 (b), showing typical alternating diurnal patterns of NH_3 emissions and dry deposition. The bi-directional, 2-layer NH_3 canopy compensation point exchange model developed by Nemitz et al. (2001) and further refined by Massad et al. (2010) was applied to the data, simulating three component fluxes (soil flux F_{soil}, stomatal flux F_{st} and non-stomatal deposition flux F_{nst}) and the resulting net canopy-scale background flux F_{bg} as the sum of the three components. The model parameters $\Gamma_{stomata}$ and Γ_{soil} (ratios of NH_4^+ to H^+ concentrations in leaf apoplast and soil water-filled pore space, respectively) were adjusted to fit the measured fluxes for each year, with $\Gamma_{stomata}$ values of 800 and 1800 in 2021 and 2022, and Γ_{soil} values of 2000 and 3000 in 2021 and 2022, respectively. The minimum resistance to non-stomatal deposition ($R_{w,\,min}$) was set to 50 s m^{-1}. See Nemitz et al. (2001) and Massad et al. (2010) for details.

Table S1: Micrometeorological screening components (% valid) of data meeting quality criteria (0 or 1) and contribution of the random error components

Period	Percentage of 0 and 1 data (%)					Random error contribution (%)	
	qcH	qcL	qc_{τ}	qc_{NH3} stationarity	$qc_{\mu met}$	u*	χ*
G1	93.3	79.6	95.6	88.8	62.2	58.4	41.6
G2	95.3	82.9	97.4	100.0	78.8	63.9	36.1
G3	96.0	87.6	98.1	99.8	83.4	32.1	67.9
G4	96.5	87.9	98.2	97.1	81.5	20.4	79.6
G5	96.3	88.2	98.1	97.9	81.9	29.2	70.8
G6	97.0	92.8	97.7	94.0	84.7	24.3	75.7
G7	96.4	94.6	99.0	93.4	84.6	41.8	58.2
G8	93.5	84.7	96.5	88.9	69.3	41.6	58.4
G9	95.6	85.7	97.5	79.4	66.8	54.1	45.9
G10	93.0	85.4	97.2	64.9	55.1	17.3	82.7

Table S2: Pearson correlation coefficients between normalized half-hourly NH_3 fluxes (scaled by daily maximum) and key environmental variables for each grazing event. Statistically significant correlations are indicated as follows: ***p < 0.001, *p < 0.01, p < 0.05; no symbol indicates p ≥ 0.05 (not significant). Air T refers to air temperature; Soil T, soil temperature; WS, windspeed; u*, friction velocity; RH, relative humidity and VPD, vapour pressure deficit.

Period	Air T (°C)	Soil T (°C)	WS (ms^{-1})	u* (ms^{-1})	RH (%)	VPD (hPa)	Rainfall (mm)
G1	-0.01	-0.19*	-0.34***	-0.18*	-0.07	0.14	-0.08
G2	-0.21	-0.37*	0.23	0.35*	0.10	-0.20	-0.15
G3	0.34***	0.10	0.25***	0.23***	-0.31***	0.33***	-0.17**
G4	0.47***	0.37***	0.31***	0.32***	-0.50***	0.52***	-0.01
G5	0.15	0.11	0.10	0.27***	-0.26***	0.28***	0.14
G6	0.35***	0.20***	0.26***	0.29***	-0.32***	0.38***	-0.03
G7	0.21*	0.11	0.48***	0.49***	-0.39***	0.31***	-0.14
G8	0.31***	0.20***	0.38***	0.38***	-0.24***	0.27***	-0.05
G9	0.50***	0.31***	0.47***	0.46***	-0.44***	0.50***	-0.13*
G10	0.14*	0.19***	-0.07	-0.05	-0.21***	0.21***	0.04

Table S3: Pearson correlation coefficients between individual half-hourly NH_3 fluxes (actual) and key environmental variables for each grazing event. Statistically significant correlations are indicated as follows: ***p < 0.001, **p < 0.01, p < 0.05; no symbol indicates p ≥ 0.05 (not significant).

Period	Air T (°C)	Soil T (°C)	WS (ms^{-1})	u* (ms^{-1})	RH (%)	VPD (hPa)	Rainfall (mm)
G1	-0.20*	-0.36***	-0.48***	-0.34***	0.11	-0.04	-0.06
G2	-0.11	-0.30	0.13	0.22	-0.04	-0.07	-0.18
G3	0.18**	-0.03	0.53***	0.30***	-0.17**	0.16**	-0.11
G4	0.25***	0.21***	-0.03	0.01	-0.25***	0.32***	-0.05
G5	0.22**	0.30***	0.13	0.39***	-0.64***	0.59***	-0.17*
G6	0.18***	0.03	0.12**	0.15**	-0.32***	0.34***	-0.04
G7	-0.07	-0.01	0.34***	0.34***	-0.18	0.08	-0.10
G8	0.37***	0.27***	0.18***	0.13*	-0.03	0.13*	-0.04
G9	0.17**	0.14*	-0.06	0.00	-0.37***	0.36***	-0.10
G10	0.20***	0.16**	0.09	0.07	-0.21***	0.27***	-0.03

S1 Soil Sampling and Analysis for mineral Nitrogen and pH

Soil samples for the determination of nitrate (NO_3^--N) and ammonium (NH_4^+-N) were collected before and after grazing from 24 points in the sampled field during 2023 and 2024. Initially (early 2023), samples were taken from the top 0-30 cm soil layer. In subsequent campaigns, sampling was stratified into three depths: 0–2, 2–15, and 15–30 cm. Composite samples were made from these, resulting in four composite samples per depth. Samples were stored in polythene bags, labelled with indelible markers, placed in a cooler, and transported to the laboratory. On arrival, soil samples were sieved through a <2 mm mesh and frozen until analysis. Mineral nitrogen (NO_3^- and NH_4^+) was determined following NF ISO 14256-2 (March 2007). A 25 g portion of moist soil was extracted with 50 mL of 1 M KCl, agitated for 30 minutes, decanted and 20 ML of supernatant was then filtered through a 0.45 µm syringe filter. The extracts were analyzed colorimetrically using a Smartchem 200 (AMS Alliance).

Soil pH was measured according to NF EN ISO 10390 (March 2022) on the <2 mm fraction using distilled deionized water 1 M KCl or 0.005 mol L^{-1} $CaCl_2$ as extractants. The soil-to-solution ratio was 1:5 (10 g dry soil mixed with 50 mL of solution).

S2 Gap-filling approach and cumulative flux estimation for grazing event

For the G9 grazing event, the normalized mean diurnal variation approach (DVmax or DVavg) described in section 2.6 could not be applied directly due to the absence of valid flux data (following quality filtering) during the first three days following grazing (D_g, D_{g+1}, D_{g+2}). To address this, a modified approach was implemented to ensure robust gap-filling while retaining consistency with the DVmax or DVavg method.

We identified the last day with the highest number of valid flux measurements before grazing and used it as a guiding reference day (D_{ref}). The daily maximum ($F_{dailyMax}(D)$) for the missing early days were estimated by interpolating between $F_{dailyMax}(D_{ref})$ and values from subsequent valid days (e.g., D_{g+3}, D_{g+4} and so on).

$$F_{dailyMax}(D_g, D_{g+1}, D_{g+2}) = Interpolated\{F_{dailyMax}(D_{ref}), F_{dailyMax}(D_{g+3}), \dots\} \quad \text{Eq. S1}$$

For events with such gaps (e.g., G10) but where the missing daily flux values were located in the middle of the grazing event. In this case, the daily statistics (eg., $F_{dailyMax}$) for the missing day were estimated by interpolating between the earlier and later valid days within the same grazing period.

A variant of the approach was also implemented using the daily average (DVavg) instead of the daily maximum. The resulting daily scaling factors were then applied using the same DVmax or DVavg framework described in section 2.6.